IOP PUBLISHING EUROPEAN JOURNAL OF PHYSICS

Eur. J. Phys. **31** (2010) 273–284 doi:10.1088/0143-0807/31/2/004

Teaching stable two-mirror resonators through the fractional Fourier transform

Ignacio Moreno[1], **Pascuala Garcia-Martinez**[2] and **Carlos Ferreira**[2]

[1] Departamento de Ciencia de Materiales, Optica y Tecnología Electrónica, Universidad Miguel Hernández, 03202 Elche, Spain
[2] Departamento de Optica, Universitat de Valencia, 45100 Burjassot, Spain

Received 23 September 2009, in final form 26 November 2009
Published 29 December 2009
Online at stacks.iop.org/EJP/31/273

Abstract

We analyse two-mirror resonators in terms of their fractional Fourier transform (FRFT) properties. We use the basic ABCD ray transfer matrix method to show how the resonator can be regarded as the cascade of two propagation–lens–propagation FRFT systems. Then, we present a connection between the geometric properties of the resonator (the g parameters) and those of the equivalent FRFT systems (the FRFT order and scaling parameters). Expressions connecting Gaussian beam q-transformation with FRFT parameters are derived. In particular, we show that the beam waist of the resonator's mode is located at the plane leading to two FRFT subsystems with equal scaling parameter which, moreover, coincides with the mode Rayleigh range. Finally we analyse the resonator's stability diagram in terms of the fractional orders of each FRFT subsystem, and the round trip propagation. The presented analysis represents an interesting link between two topics (optical resonators and Fourier optics) usually covered in optics and photonics courses at university level, which can be useful to teach and connect the principles of these subjects.

1. Introduction

Laser resonators are key optical components, included in all modern optics and photonics courses for Physics or Engineering degrees. After the initial works in the 1960s [1], it became a subject actually included in all textbooks in the field of optics [2, 3]. Typically two types of analyses are employed for its study. A first one is based on geometrical optics considerations, where the stability of the ray trajectories inside the cavity is analysed. A second and more complete analysis is based on wave optics theory and permits the derivation of the propagation modes of the resonators. In spite of being a widely studied subject, there is still interest in the comprehension of their physical insights [4].

Another field of interest since its introduction in optics in 1993 by Mendlovic and Ozatkas [5] is the fractional Fourier transform (FRFT). This operation is the generalization to fractional orders of the Fourier transform, and much research has been conducted to use the FRFT for the analysis of optical systems. In particular, pretty soon the FRFT was recognized as a powerful tool to analyse optical resonators since they share Hermite–Gaussian functions as eigenfunctions [6, 7]. The general relationships between ray optics, Gaussian beams and FRFT systems were further explored in [8]. Both mirror resonators and FRFT systems are paraxial first-order systems, and therefore can be analysed in a very elegant and compact way through the ABCD ray transfer matrix method [9]. In mirror resonators, this formalism is typically employed to analyse ray confinement and develop the stability diagram [3]. The properties of the ABCD matrix of FRFT systems have been studied for instance in [10, 11], and it has been shown to be especially useful to establish connections with geometrical optics aspects of FRFT optical systems [12, 13]. The simplicity of ray matrices as compared to diffraction integrals permits teaching in a simple manner several topics of Fourier optics theory, including the FRFT systems [11].

In this paper, we follow that line and take a step further, where we apply the ABCD ray matrix to analyse stable resonators in terms of FRFT properties. The existing close connection between the FRFT operation and optical resonators has been established in the previous advanced references [6, 14–16]. In [6], the FRFT property of the resonator round trip propagation was identified, and symmetrical resonators were analysed. In [14], general multi-element resonators were analysed by considering two single pass (forward and backward) propagations. In [15, 16], the FRFT relation between the light amplitude distributions at spherical surfaces was established on the basis of scalar diffraction, and the conclusions were applied to spherical resonators. In these previous related works, the FRFT property has been established either for the round trip propagation or for the mirror to mirror propagation. The novelty of our approach is that we identify the round trip propagation as the cascade of two equivalent FRFT propagation–lens–propagation subsystems like those proposed by Lohmann in [17]. The plane containing the waist of the resonator's Gaussian mode is selected as the initial propagation plane. This permits applying the general waist-to-waist propagation FRFT properties [18]. As a result, we show in a very simple manner that spherical resonators can be viewed as the cascade of two FRFT subsystems with matched scaling parameters, which in addition coincide with the Rayleigh range of the corresponding Gaussian mode. The whole derivation is presented in terms of the ABCD ray transfer matrix, thus reducing the complexity of derivations involving diffraction integral calculations. Therefore, this approach can be especially appropriate to teach the subject to undergraduate students who have been trained in ABCD matrices and in Fourier optics.

The paper is organized as follows. In section 2, we briefly review some of the relevant properties of Gaussian beams and FRFT optical systems in terms of ABCD matrix representation. In section 3, we connect these two elements to extract the FRFT properties of the mirror resonators, including a new perspective of the resonator's stability diagram in terms of the basic FRFT orders. Some particularly relevant cases are analysed in section 4. Finally, section 5 presents the conclusion of the work.

2. Ray matrices, Gaussian beams and FRFT systems

We consider regular centred rotationally symmetric geometrical optical systems working under the paraxial approximation. In this approximation, optical systems can be described by an

ABCD ray matrix:

$$\mathbf{M} = \begin{pmatrix} A & B \\ C & D \end{pmatrix}, \tag{1}$$

which relates the height and angle coordinates of the rays at the input and output planes [9, 11]. In the usual situation with air at both extremes, the determinant of the ray matrix is $\det(\mathbf{M}) = AD - CB = 1$. The ray matrix formalism is a very powerful tool to analyse optical systems, and its mathematical simplicity makes it very useful also for educational purposes. For instance, the analysis of the ray matrix permits direct derivation of geometrical properties of the optical systems: the C parameter directly gives the optical power of the system, while the imaging condition (input and output planes are conjugated) is directly obtained by imposing the condition $B = 0$ [9].

We recently proposed the use of the ray matrix formalism also to analyse Fourier optics systems [11]. Optical systems providing an exact Fourier transform relation between the wavefront's amplitude at the input and output planes can be very easily identified since the ray matrix A and D parameters become null. An exact FRFT optical system can also be very easily identified through the condition $A = D$, the fractional order p being directly related to these two parameters as $\cos(p\pi/2) = A = D$. In [11], we showed various examples that expressed the simplicity of this ray matrix analysis. Here we extend our previous work and employ this formalism to revisit stable optical resonators through their FRFT properties, which can be a very interesting and valuable educational tool since the involved calculations are very simple compared to the standard diffraction integrals.

2.1. Gaussian beams and waist-to-waist propagation

Gaussian beams are introduced in many optics and photonics basic texts since they are the fundamental modes of optical resonators [1–3]. They are described mathematically by the wavefront:

$$a(\mathbf{r}) = \frac{A}{q(z)} \exp\left(-\mathrm{i}k \frac{\rho^2}{2q(z)}\right), \tag{2}$$

where $\mathbf{r} = (x, y, z)$ (the beam is assumed to propagate along the z axis) and $k = 2\pi/\lambda$. The q-parameter is defined as

$$\frac{1}{q(z)} = \frac{1}{z + \mathrm{i}z_R} = \frac{1}{R(z)} - \mathrm{i}\frac{\lambda}{\pi w^2(z)}, \tag{3}$$

z_R being the Rayleigh range. $R(z)$ and $w(z)$ are respectively the radius of curvature and beam width (spot size) at the plane z, and they are given by

$$R(z) = z\left(1 + \left(\frac{z_R}{z}\right)^2\right), \tag{4}$$

$$w(z) = w_0\sqrt{1 + \left(\frac{z}{z_R}\right)^2}. \tag{5}$$

The beam waist is located at $z = 0$, where the spot size is given by

$$w_0 = \sqrt{\frac{\lambda z_R}{\pi}}. \tag{6}$$

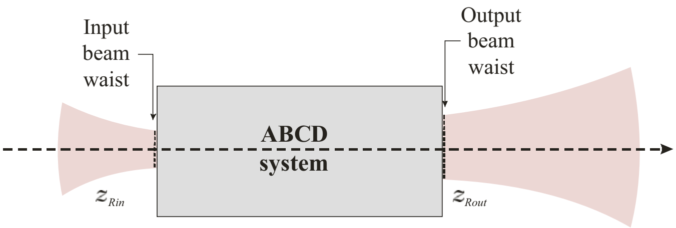

Figure 1. Optical system performing a Gaussian beam waist-to-waist transformation.

When a Gaussian beam propagates through such a system described with an ABCD ray matrix (equation (1)), the output q-parameter (q_{out}) is related to the input q-parameter (q_{in}) by

$$q_{\text{out}} = \frac{Aq_{\text{in}} + B}{Cq_{\text{in}} + D}. \tag{7}$$

At the beam waist the q-parameter is purely imaginary:

$$\frac{1}{q} = \frac{1}{\mathrm{i}z_R} = -\mathrm{i}\frac{\lambda}{\pi w_0^2}. \tag{8}$$

Here, we consider an optical system producing a waist-to-waist propagation between its input and output planes (figure 1), where the input and output planes are characterized by $q_{\text{in}} = \mathrm{i}z_{\text{Rin}}$ and $q_{\text{out}} = \mathrm{i}z_{\text{Rout}}$ respectively (z_{Rin} and z_{Rout} denote the corresponding Rayleigh ranges). Imposing the waist-to-waist propagation on equation (7) directly leads to the conclusion that such transformation is produced provided the optical system fulfils the following matching condition:

$$\frac{BD}{AC} = -z_{\text{Rin}}^2. \tag{9}$$

Then, the Rayleigh ranges of the input and output beams are related as

$$z_{\text{Rout}} = z_{\text{Rin}}\frac{A}{D}. \tag{10}$$

2.2. FRFT properties of the waist-to-waist Gaussian beam propagation

The ABCD ray matrix of an optical system performing an exact FRFT between the input and output planes is given by [10, 11]

$$\mathbf{M}_{\mathbf{FRFT}}(p,s) = \begin{pmatrix} \cos(\phi) & s\sin(\phi) \\ -\frac{1}{s}\sin(\phi) & \cos(\phi) \end{pmatrix}, \tag{11}$$

where p denotes the FRFT order, given by $\phi = p\pi/2$ and s is a scaling factor. Therefore, an optical system with ray matrix parameters $A = D$ in the range $(-1, +1)$ performs a real valued exact FRFT relationship between input and output field amplitudes [11], the fractional order p ranging from 0 to 4 (the FRFT operation shows periodicity of 4).

If a Gaussian beam propagates through a FRFT system, equation (7) indicates that the transformation for its q-parameter is

$$q_{\text{out}} = \frac{\cos\phi \cdot q_{\text{in}} + s\sin\phi}{-\frac{1}{s}\sin\phi \cdot q_{\text{in}} + \cos\phi}. \tag{12}$$

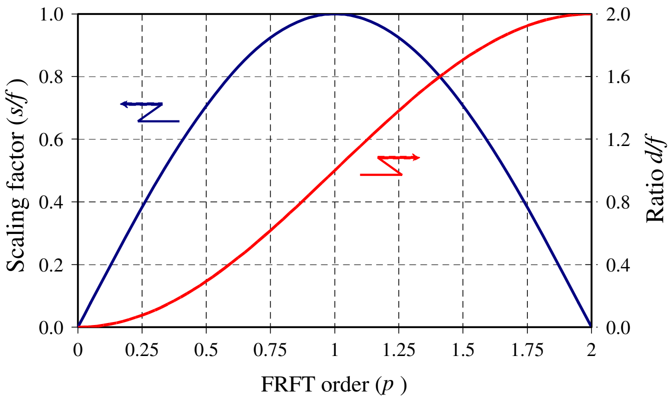

Figure 2. Evolution of the normalized scaling factor s/f and the ratio d/f as a function of the FRFT order (p) in a Lohmann propagation–lens–propagation system.

If, in addition, the FRFT system performs a waist-to-waist propagation, equations (9)–(11) lead to the following condition (up to a sign):

$$z_{\mathrm{Rout}} = z_{\mathrm{Rin}} = s. \tag{13}$$

This equation shows a very interesting conclusion: if an exact FRFT system performs a waist-to-waist transformation on a Gaussian beam, then the Rayleigh range is conserved and it must be equal to the FRFT scaling factor. In the next section we will use this property to analyse stable two-mirror resonators.

One of the basic FRFT bulk lens systems was proposed by Lohmann in [17], consisting in a propagation–lens–propagation system, where the propagations on either side of the lens are of equal distance d. If f denotes the lens focal length, the ray matrix for such a system is given by [11]

$$\mathbf{M}_{\mathbf{FRFT}}(p, s) = \begin{pmatrix} 1 - \dfrac{d}{f} & d\left(2 - \dfrac{d}{f}\right) \\ -\dfrac{1}{f} & 1 - \dfrac{d}{f} \end{pmatrix}. \tag{14}$$

The comparison with equation (11) reveals that this system provides a real valued FRFT when the distance d is between 0 and $2f$, the fractional order p being given by the relation

$$\cos\left(p\frac{\pi}{2}\right) = 1 - \frac{d}{f}. \tag{15}$$

Moreover, the FRFT scaling factor is given by the relation

$$s^2 = d(2f - d). \tag{16}$$

Figure 2 shows the evolution of the scaling factor normalized to the lens focal length (s/f), as well as the required propagation distance to focal length ratio (d/f) as a function of the required FRFT order (p). The scaling parameter becomes null at the extreme values ($p = 0$ and $p = 2$), while it reaches a maximum value for the Fourier transform system ($p = 1$). The ratio d/f increases nonlinearly but monotonically as the FRFT order increases.

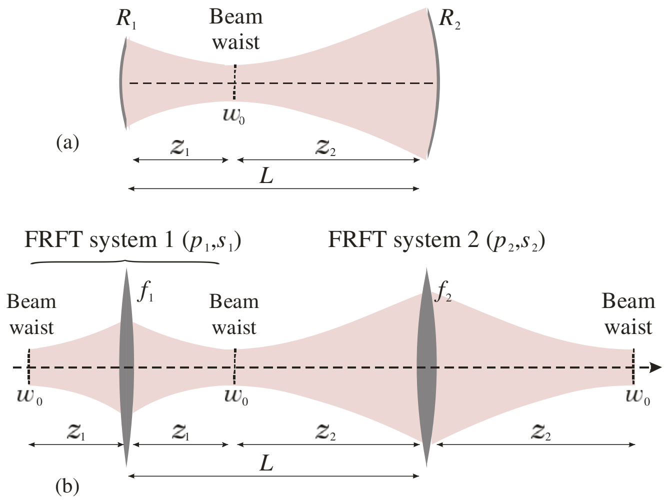

Figure 3. (a) Scheme of the optical resonator and its Gaussian mode. (b) Equivalent system composed of two Lohmann FRFT systems.

3. FRFT properties of optical resonators

We next exploit all these results for the analysis of optical stable resonators. While some FRFT properties of resonators have been investigated in previous works [6, 7, 14–16], here we adopt a different point of view related to the previous Lohmann FRFT lens system [17]. Figure 3(a) shows a scheme of the two-mirror resonator, where the corresponding Gaussian mode is drawn. There are two parameters of interest to characterize the resonator mode: (1) the location of the beam waist and (2) the value of the Rayleigh range (z_R). From figure 3(a), the waist plane is described by either distance z_1 or z_2. Other beam parameters—the spot size at the waist plane (w_0) and at the two mirrors (w_1 and w_2), and the radii of curvature at the mirrors ($R(z_1)$ and $R(z_2)$)—can be calculated from the Rayleigh range z_R through equations (3)–(5). A usual derivation of such parameters is obtained by imposing a matching condition among the wavefronts and mirror curvatures [2, 3].

In this work we propose an alternative derivation, where we focus on the waist-to-waist propagation (through a mirror reflection). To avoid the use of uncomfortable sign change conventions for the mirror reflections, and to directly compare with the FRFT lens system proposed by Lohmann, we consider the two-mirror resonator as an equivalent lens system drawn in figure 1(b), where the mirrors have been replaced by two lenses with focal lengths $f_1 = R_1/2$ and $f_2 = R_2/2$, R_1 and R_2 being the radii of curvature of the mirrors. This figure clearly shows that the round trip propagation in the resonator can be viewed as the propagation along two Lohmann type FRFT systems, both with the origin at the beam waist. We next derive the relation between the geometrical and FRFT parameters of such Lohmann type subsystems. For that purpose we consider the two following conditions.

(1) The total length between the lenses must be equal to the resonator length: $z_1 + z_2 = L$.

(2) The beam width at the three beam waists shown in figure 1(b) must be the same (w_0) since they all correspond to the same Gaussian mode and because of that there is only a single beam waist propagating in the resonator.

Imposing the conservation of w_0 at the three waists drawn in figure 3(b), and taking into account equation (13), it is direct to conclude that the two FRFT subsystems must share the same scaling factor, which in addition must be equal to the Rayleigh range of the Gaussian mode, i.e.

$$s_1 = s_2 = z_R. \tag{17}$$

Therefore, we can highlight the following interesting result: a two-mirror resonator can be regarded as the cascade of two FRFT systems with identical scaling factor, and the Gaussian beam mode matching the resonator is defined by a Rayleigh range equal to this FRFT scaling factor.

Therefore, the ABCD ray matrix of the two FRFT subsystems composing the optical resonator can be written as

$$\mathbf{M_{FRFT}}(p_i, z_R) = \begin{pmatrix} \cos(\phi_i) & z_R \sin(\phi_i) \\ -\dfrac{1}{z_R}\sin(\phi_i) & \cos(\phi_i) \end{pmatrix}, \tag{18}$$

where $i = 1, 2$ denote each of the two FRFT subsystems, and where p_i denote the corresponding FRFT orders, which are related to the resonator geometrical parameters through equation (15) as

$$\cos(\phi_i) = \cos\left(p_i \frac{\pi}{2}\right) = 1 - \frac{z_i}{f_i}. \tag{19}$$

The Rayleigh range of the Gaussian beam can be directly derived from equation (16), being

$$z_R^2 = z_1\,(2f_1 - z_1) = z_2\,(2f_2 - z_2)\,. \tag{20}$$

The above equation gives another important connection between the Gaussian beam propagation and FRFT analysis. The location of the beam waist can be easily derived from the FRFT analysis by combining this previous scaling matching condition (equation (20)) with the condition $z_1 + z_2 = L$, leading to

$$z_1 = \frac{L}{2} \cdot \frac{2f_2 - L}{f_1 + f_2 - L}; \qquad z_2 = \frac{L}{2} \cdot \frac{2f_1 - L}{f_1 + f_2 - L}. \tag{21}$$

These relations provide the location of the beam waist of the Gaussian beam mode of the resonator in terms of its geometrical parameters (L, f_1 and f_2), and they are usually derived otherwise by imposing the beam curvature matching condition [2, 3].

The ray matrix ($\mathbf{M_{RT}}$) corresponding to a round trip (RT) propagation in the resonator is obtained by multiplying those corresponding to the two FRFT subsystems, i.e.

$$\begin{aligned} \mathbf{M_{RT}} &= \mathbf{M_{FRFT}}(p_2, z_R) \cdot \mathbf{M_{FRFT}}(p_1, z_R) \\ &= \begin{pmatrix} \cos(\phi_2)\cos(\phi_1) - \sin(\phi_2)\sin(\phi_1) & z_R[\cos(\phi_2)\sin(\phi_1) + \sin(\phi_2)\cos(\phi_1)] \\ -\dfrac{1}{z_R}[\cos(\phi_2)\sin(\phi_1) + \sin(\phi_2)\cos(\phi_1)] & \cos(\phi_2)\cos(\phi_1) - \sin(\phi_2)\sin(\phi_1) \end{pmatrix} \\ &= \begin{pmatrix} \cos(\phi) & z_R\sin(\phi) \\ -\dfrac{1}{z_R}\sin(\phi) & \cos(\phi) \end{pmatrix} = \mathbf{M_{FRFT}}(p_1 + p_2, z_R), \end{aligned} \tag{22}$$

where $\phi = \phi_1 + \phi_2 = (p_1 + p_2)\pi/2$. This equation reveals an expected result: the round trip propagation is another FRFT system, with the same scaling parameter as of each FRFT subsystem, equal to the Rayleigh range of the corresponding Gaussian beam. The FRFT order of the round trip is the addition of the orders of each subsystem ($p = p_1 + p_2$). But we find it important to note that this property is obtained since $\mathbf{M_{RT}}$ in equation (22) can be written as a FRFT ray matrix because both FRFT subsystems share the same scaled variables.

The explicit calculation of the matrix $\mathbf{M_{RT}}$ in terms of f_1, f_2 and L reveals that the A element of the matrix in equation (22) is given by [3]

$$\cos(\phi) = 1 - L\left(\frac{1}{f_1} + \frac{1}{f_2}\right) + \frac{L^2}{2f_1 f_2}. \tag{23}$$

Real values for the FRFT order after a round trip are obtained if $-1 \leqslant \cos(\phi) \leqslant +1$. This condition (as was already derived in previous works [6, 16]) is equivalent to the resonators' stability condition. This is usually analysed in terms of the resonators' g-parameters, defined as

$$g_i = 1 - \frac{L}{2f_i}. \tag{24}$$

Equation (23) can be rewritten as

$$\cos^2\left(\frac{\phi}{2}\right) = g_1 g_2, \tag{25}$$

where $\phi = p\pi/2$, p being the FRFT order of the round trip propagation. This equation shows the equivalence among real valued FRFT orders and the resonators' stability condition ($0 \leqslant g_1 g_2 \leqslant 1$). As pointed out in [16], complex order FRFT correspond to unstable optical resonators, where propagation fades out due to diffraction losses.

Furthermore, the round trip FRFT order (p) defines some interesting graphic lines in the stability diagram. Figure 4 shows this diagram, where we have indicated some examples. The extreme cases $g_1 g_2 = 1$ correspond to FRFT orders $p = 0$ or $p = 4$. These are two special cases where the field after the round trip is a direct (non-inverted) output image of the input field. The axes of the diagram, $g_1 = 0$ and $g_2 = 0$, correspond to a FRFT order $p = 2$, i.e. after a round trip an inverted output image of the input field is obtained.

Figure 4(a) also shows two (red) curves, which correspond to Fourier transforming systems ($p = \pm 1$), obtained after the condition $g_1 g_2 = 1/2$. Each round trip in a resonator lying in these lines provides a Fourier transform between the input and output beams. The condition $g_1 g_2 = 1/2$ corresponds to a direct Fourier transformation when the g-parameters are positive, while it provides an inverse Fourier transform when the g-parameters are negative. Two other straight lines have been drawn in figure 4(a), corresponding respectively to the symmetric resonators (diagonal line $g_1 = g_2$), and to the half-symmetric resonators ($g_1 = 1$ or $g_2 = 1$), which are analysed in detail in the next section.

In general, each FRFT subsystem contributes differently to the round trip FRFT order. In order to calculate this contribution, it is useful to first write the distances z_1 and z_2 in terms of the g-parameters as [2]

$$z_1 = L \cdot \frac{g_2(1-g_1)}{g_1 + g_2 - 2g_1 g_2}; \qquad z_2 = L \cdot \frac{g_1(1-g_2)}{g_1 + g_2 - 2g_1 g_2}. \tag{26}$$

Then, their combination with equation (19) leads to the following expressions of the orders of each FRFT subsystem (p_1 and p_2) in terms of the geometrical parameters (g_1 and g_2):

$$\cos\left(p_1 \frac{\pi}{2}\right) = 1 - \frac{2g_2(1-g_1)^2}{g_1 + g_2 - 2g_1 g_2}; \qquad \cos\left(p_2 \frac{\pi}{2}\right) = 1 - \frac{2g_1(1-g_2)^2}{g_1 + g_2 - 2g_1 g_2}. \tag{27}$$

Figures 4(b) and (c) represent respectively p_1 and p_2 in the stability diagram, where we draw them in the range $[-2, +2]$ for the sake of clarity by providing a continuity of the curves. The FRFT orders in the round trip propagation shown in figure 4(a) are obtained as the pointwise addition of the FRFT orders in figures 4(b) and (c). These two figures are symmetrical to each other around the diagonal line corresponding to the symmetrical resonators ($g_1 = g_2$).

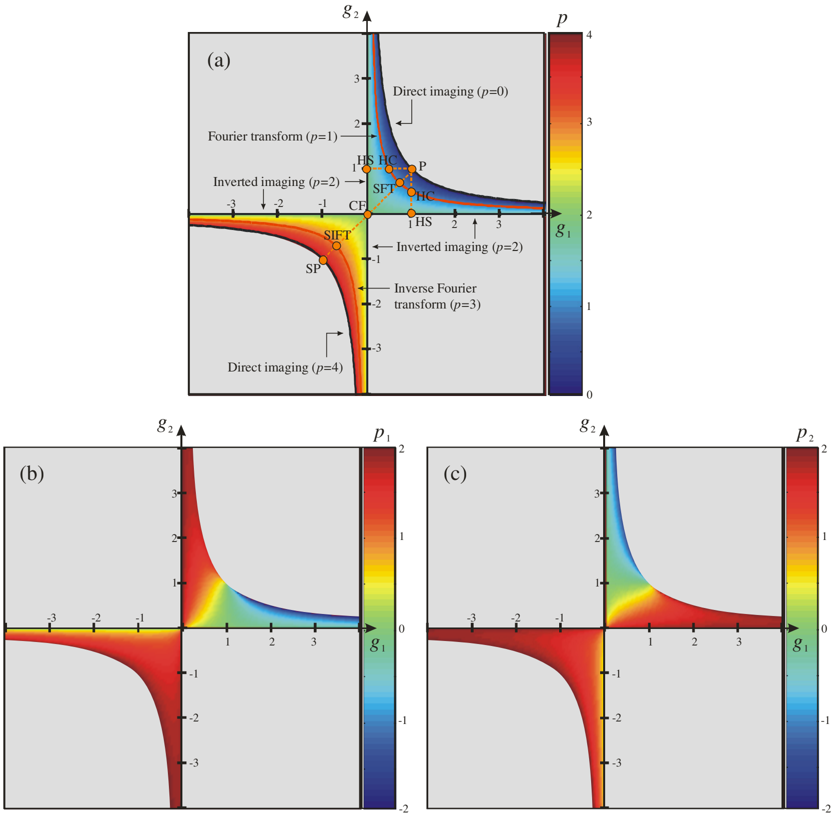

Figure 4. (a) Resonator's stability diagram and identification of FRFT curves. Some well-known resonators are indicated: P: planar; CF; confocal; SP: spherical; HC: hemi-confocal; HS: hemi-spherical; SFT: symmetrical direct Fourier transform resonator; SIFT: symmetrical inverse Fourier transform resonator. The FRFT orders of each subsystem are represented in the diagram in (b) p_1 and (c) p_2.

Finally, it is interesting to rewrite the Gaussian beam parameters (w_0, w_1 and w_2) in terms of the g-parameters as [2]

$$w_0^2 = \frac{\lambda z_R}{\pi} = \frac{L\lambda}{\pi}\sqrt{\frac{g_1 g_2(1-g_1 g_2)}{(g_1+g_2-2g_1 g_2)^2}}, \tag{28}$$

$$w_1^2 = \frac{L\lambda}{\pi}\sqrt{\frac{g_2}{g_1(1-g_1 g_2)}}, \qquad w_2^2 = \frac{L\lambda}{\pi}\sqrt{\frac{g_1}{g_2(1-g_1 g_2)}}. \tag{29}$$

These parameters are connected to each FRFT order through equations (27).

4. FRFT analysis of some particular resonators

4.1. Symmetric resonators

We consider next the simplest case: symmetric resonators, i.e. $f_1 = f_2$. They can be described by a single geometrical parameter $g_1 = g_2 \equiv g$, the beam waist is located at the centre of the

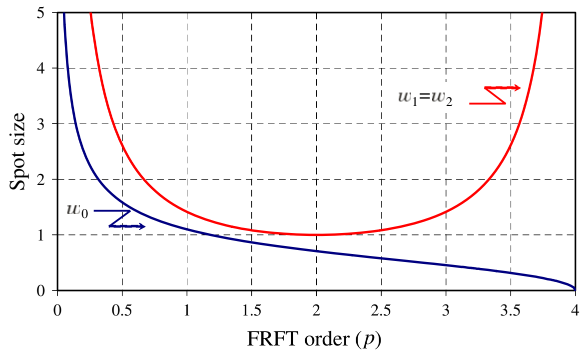

Figure 5. Evolution of the beam spot size at the beam waist (w_0) and at the two mirrors (w_1 and w_2) as a function of the round trip FRFT order in a symmetric resonator. The spot size is represented in units of $\sqrt{L\lambda/\pi}$.

resonator ($z_1 = z_2 = L/2$) and the two FRFT subsystems are identical $p_1 = p_2 = p/2$. They lie on the diagonal line in the stability diagram. Equation (25) reveals the following simple connection between g and p:

$$\cos^2\left(p\frac{\pi}{4}\right) = g^2. \tag{30}$$

As g^2 continuously varies from 1 to 0, p continuously varies from 0 to 2 (in the positive g quadrant) and from 4 to 2 (in the negative g quadrant). The well-known planar (P), confocal (CF) and spherical (SP) resonators correspond to $p = 0$, 2 and 4, respectively. Two other symmetrical resonators are marked in figure 4, the symmetrical direct (SDFT) and symmetrical inverse (SIFT) Fourier transform resonators. They correspond to $g = \pm 1/\sqrt{2}$, and to orders $p = 1$ and $p = 3$, respectively. In the first case ($p = 1$), each FRFT subsystem performs transformations of order $p_1 = p_2 = 1/2$, while in the second case ($p = 3$), they perform FRFT of orders $p_1 = p_2 = 3/2$.

For the symmetrical resonators, equations (28)–(30) provide the following connection between the Gaussian beam parameters and the round trip FRFT order (expressed in terms of the phase $\phi = p\pi/2$):

$$w_0^2 = \frac{L\lambda}{\pi}\cdot\frac{1}{2\tan(\phi/4)} \tag{31}$$

$$w_1^2 = w_2^2 = \frac{L\lambda}{\pi}\cdot\frac{1}{\sin(\phi/2)}. \tag{32}$$

Figure 5 shows the evolution of the spot size at the waist (w_0) and at the two mirrors (w_1 and w_2) as a function of the FRFT order p. The transition from $p = 0$ to $p = 4$ corresponds to transit along the diagonal line drawn in figure 4(a). Figure 5 shows that the w_0 monotonically decreases as p increases, while $w_1 = w_2$ has the minimum value for $p = 2$, and diverges at the limits $p = 0$ and $p = 4$.

4.2. Half-symmetric resonators

Half-symmetric resonators are defined by using one planar mirror. The waist is located on the planar mirror, and all the FRFT transformation is achieved by the waist-to-waist propagation

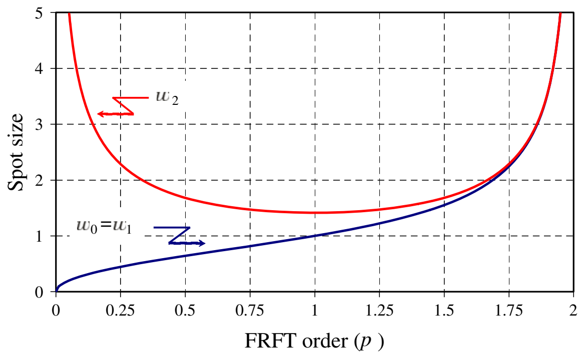

Figure 6. Evolution of the beam spot size at the beam waist (w_0) and at the two mirrors (w_1 and w_2) as a function of the round trip FRFT order in a half-symmetric resonator. The spot size is represented in units of $\sqrt{L\lambda/\pi}$.

through the other curved mirror. The lines in the stability diagram corresponding to these resonators ($g_1 = 1$ or $g_2 = 1$) present a null contribution on the order of the FRFT subsystem with the planar mirror (p_1 in figure 4(b) and p_2 in figure 4(c)). The round trip propagation can be regarded as a single Lohmann FRFT system. The resonator stability is described with the g-parameter corresponding to the curved mirror, which is related to p through equation (25) which now adopts the form

$$\cos^2\left(p\frac{\pi}{4}\right) = g. \tag{33}$$

Finally, the Gaussian beam spot size is now related to p through equations (28) and (29) as

$$w_0^2 = w_1^2 = \frac{L\lambda}{\pi} \cdot \frac{1}{\tan(\phi/2)}, \tag{34}$$

$$w_2^2 = \frac{L\lambda}{\pi} \cdot \frac{2}{\sin(\phi)}, \tag{35}$$

where again $\phi = p\pi/2$. Figure 6 shows the evolution of the spot size as a function of the FRFT order. Now we plot the graph in the range $p \in [0–2]$, which corresponds to a transit along the vertical line $g_1 = 1$ in the stability diagram in figure 4(a). Now, $w_0 = w_1$ monotonically increases with p, while w_2 has the minimum value for $p = 1$, and diverges for $p = 0$ and $p = 2$.

5. Conclusions

In summary, we have provided an analysis of stable two-mirror resonators based on their analogy as two cascaded propagation–lens–propagation FRFT systems. The complete derivation is based on the use of a simple ABCD ray matrix formalism, and provides relevant equations connecting Gaussian resonator mode q-parameter with the FRFT parameters. Two main conclusions that we identified are (1) the two propagation–lens–propagation FRFT subsystems composing the resonator must share the same scaling parameter; (2) the Rayleigh range of the Gaussian beam mode of the resonator also equals this FRFT scaling factor. Moreover, using the simple mathematics of ray matrices, we reach the same conclusions as other previous FRFT studies in which the application to optical resonators may be more tedious, as we referred to in the text.

Based on this point of view, we analysed the resonators' stability diagram, and we have identified different lines defining the different FRFT orders. We derived the equations relating the spot size of the resonators Gaussian modes to the FRFT orders, which adopt a particular form depending on the particular configuration. Some very well known particular cases (symmetrical and half-symmetrical resonators) have been analysed in more detail, providing analytical relations between the geometrical parameters (g) and the FRFT order (p).

The presented analysis represents a FRFT-based point of view for studying mirror resonators that complements and relates the usual treatments based either on pure geometrical optics analysis (stability of the ray trajectories) or on the wave optics analysis (that provides the modes of the resonators). Thus, this point of view can be very interesting for optics and photonics courses since it is suitable for teaching and linking optical FRFT systems, Gaussian beams and resonators. The equations and systems shown in the last two sections can be used for an excellent theoretical training for learning two-mirror resonators.

Acknowledgments

This work was supported by Fondo Europeo de Desarrollo Regional (FEDER) and the Spanish Ministerio de Ciencia e Innovación (projects FIS2009-13955-C02-02 and FIS2007-60626).

References

[1] Kogelnik H and Li T 1966 Laser beams and resonators *Appl. Opt.* **5** 1550–67
[2] Siegman A E 1986 *Lasers* (Sausalito: University Science Books)
[3] Saleh B E A and Teach M 1991 Resonator optics *Fundamentals of Photonics* (New York: Wiley) Chapter 9
[4] Forrester A, Lönnqvist M, Padgett M J and Courtial J 2002 Why are the eigenmodes of a stable laser resonator structurally stable? *Opt. Lett.* **27** 1869–71
[5] Mendlovic D and Ozatkas H M 1993 Fractional Fourier transform and their optical implementation I *J. Opt. Soc. Am.* A **10** 1875–81
[6] Ozatkas H M and Mendlovic D 1994 Fractional Fourier transform as a tool for analyzing beam propagation and spherical mirror resonators *Opt. Lett.* **19** 1678–80
[7] Ozatkas H M, Zalevsky Z and Kutay M A 2000 Hermite–Gaussian expansion approach *The Fractional Fourier Transform with Applications in Optics and Signal Processing* (Chichester: Wiley) section 9.6
[8] Ozatkas H M and Erden M F 1997 Relationships among ray optical, Gaussian beam, and fractional Fourier transform descriptions of the first-order optical systems *Opt. Commun.* **143** 75–86
[9] Kloos G 2007 *Matrix Methods for Optical Layout* (Bellingham: SPIE Press)
[10] Bernardo L M 1996 ABCD matrix formalism of fractional Fourier optics *Opt. Eng.* **35** 732–40
[11] Moreno I, Sánchez-López M M, Ferreira C, Davis J A and Mateos F 2005 Teaching Fourier optics through ray matrices *Eur. J. Phys.* **26** 261–71
[12] Moreno I, Sánchez-López M M, Ferreira C and Mateos F 2007 Fractional Fourier transform, symmetrical lens systems and its cardinal planes *J. Opt. Soc. Am.* A **24** 1930–6
[13] Moreno I, Ferreira C and Sánchez López M M 2006 Ray matrix analysis of anamorphic fractional Fourier systems *J. Opt. A: Pure Appl. Opt.* **8** 427–35
[14] Zhao D 1999 Multi-element resonators and scaled fractional Fourier transforms *Opt. Commun.* **168** 85–8
[15] Hwang H E and Han P 2005 Fractional Fourier transform optimization approach for analyzing optical beam propagation between two spherical surfaces *Opt. Commun.* **245** 11–9
[16] Pellat-Finet P and Fogret E 2006 Complex order fractional Fourier transforms and their use in diffraction theory. Application to optical resonators *Opt. Commun.* **258** 103–13
[17] Lohmann A W 1993 Image rotation, Wigner rotation and the fractional Fourier transform *J. Opt. Soc. Am.* A **10** 2181–6
[18] Ge F, Wang S and Zhao D 2007 The representation of waist-to-waist transformation of Gaussian beams by the scaled fractional Fourier transform *Opt. Lasers Eng.* **39** 831–4